RSC Advances

ROYAL SOCIETY OF CHEMISTRY

www.rsc.org/advances

Cite this: DOI: 10.1039/c0xx00000x

www.rsc.org/xxxxxx

ARTICLE TYPE

A novel pyrene-2-(pyridin-2-ylmethylsulfanyl)ethylamine based turn-on dual sensor for Al^{3+}: experimental and computational studies†

Rahul Bhowmick[a], Malay Dolai[a], Rabiul Alam[a], Tarun Mistri[a], Atul Katarkar[b], Keya Chaudhuri[b] and Mahammad Ali[a]*

Received (in XXX, XXX) Xth XXXXXXXXX 200X, Accepted Xth XXXXXXXXX 200X
DOI: 10.1039/b000000x

A new pyrene based highly sensitive and selective Al^{3+} sensor, pyrene-2-(Pyridin-2-ylmethylsulfanyl)-ethylamine (PP), was found to exhibit a turn-on fluorescence enhancement (FE) as high as 7.4 fold with K_d (2.55 ± 0.10) x 10^{-4} M and n =1. Not only that this probe binds reversibly towards Al^{3+} in presence of H_2EDTA^{2-} , both in intra- and exctracellular conditions. LOD determined by 3σ methods was found to be 15 nM while LOQ = 52.8 nM. The tentative coordination environment in the Al^{3+}-PP complex was delineated by DFT calculations both on the free ligand and complex. The TDDFT calculations reveal the spectral features comparable to the experimental ones.

Introduction

Fluorescent chemosensor is a growing field of research and attracting the interest of chemists, biologists and environmental scientists owing to their potential applications in medicinal and environmental research. Thus, many fluorescent chemosensors for heavy metal ions like Zn^{2+}, Cd^{2+} and Hg^{2+}, and for many transitions metal ions have been developed in recent years. The detection of Al^{3+} has always been a problematic task due to the lack of spectroscopic characteristics and poor coordination ability.[1] In addition, most of the reported Al^{3+} sensors are insoluble in aqueous medium and require complicated synthetic procedures. For practical applications, it is necessary to develop Al^{3+} sensors that are easily prepared and possess selective and sensitive signalling mechanisms. Compared to other metal ions, only a few fluorescent chemosensors have been reported for the detection of Al^{3+},.[2-7]

Despite of being a non-essential element, the detection of Al^{3+} is of great interest due to its potential toxicity arising out of its widespread application in automobiles, computers, packaging materials, electrical equipment, machinery food additives building construction, clinical drugs and water purification.[8,9] Furthermore, it is well known that 40% of soil acidity is due to aluminium toxicity.[10]

Department of Chemistry Jadavpur University, Kolkata 700 032, India; Fax: 91-33-2414-6223, E-mail: mali@chemistry.jdvu.ac.in

† Electronic Supplementary Information (ESI) available: See DOI: 10.1039/b000000x/of

Aluminium leaching from soil by acid rain is deadly to growing plants.[11] The World Health Organization (WHO) prescribed the average human intake of aluminium is ~ 3–10 mg day^{-1} with a weekly dietary intake of 7 mg day^{-1} body weight.[12] Aluminium toxicity damages the central nervous system and it is suspected of playing a role in neurodegenerative Alzheimer and Parkinson diseases. It is also responsible for intoxication in haemodialysis patients.[13] Therefore, detection of Al^{3+} is crucial in controlling its concentration levels in the biosphere and its direct impact on human health.

A number of high-end techniques available for Al^{3+} estimation includes chromatography[14], accelerator mass spectroscopy (AMS)[15] , graphite furnace atomic absorption spectrometry (GFAAS)[16] , neutron activation analysis (NAA)[17], inductively coupled plasma-atomic emission spectrometry (ICP-AES)[18], inductively coupled plasma-mass spectrometry (ICP-MS)[19], laser ablation microprobe mass analysis (LAMMA)[20], electrothermal atomic absorption spectrometry (ETAAS)[21] etc but most of them require sophisticated instruments and time consuming for sample preparation protocols and cost-effective too. On the contrary, fluorescence chemosensors are the best choices, as it is the simplest, sensitive, fast and inexpensive technique[22] offering significant advantages over other methods.[23] Hence, recently the design and synthesis of Al^{3+} selective fluorescent probes has received intense attention of the chemists.[24,25,26]

Most of the reported Al^{3+} sensors suffer from interference of Fe^{3+} and Cu^{2+} and require tedious synthetic methodology.[27] Al^{3+} being hard acid prefers to bind with hard bases and consequently most of the Al^{3+} probes are found to coordinate with hard donor atoms like N and O. However, the strong binding of a receptor to an analyte may lead to lose selectivity as well as reversibility, which are essential for practical applications. There are a few reports where a soft donor atom like S

has been introduced for the recognition of Al^{3+}.[28] The probes with such soft donor atoms may recognise a hard metal ion with enhanced selectivity over the other competing guests.[29] Here we are reporting a highly selective Al^{3+} probe containing N_2S donor atoms that binds selectively to Al^{3+} in presence of other metal ions. The coordination environment around the metal ion in Al^{3+}-PP complex was delineated by DFT calculations both on the free ligand and its Al^{3+} complex.

Results and Discussion

(Pyridin-2-ylmethylsulfanyl)-ethylamine(P) was synthesized as outlined inScheme 1.[30] The probe (**PP**) was then prepared by a simple Schiff base condensation between P and pyrene-2-aldehyde in EtOH. This ligand is suitable for Al^{3+} recognition and characterized by NMR (**Fig.S1, S2 and S3**), mass analysis (**Fig.S4, S5 and S6**) and IR analysis (**Fig. S7**).

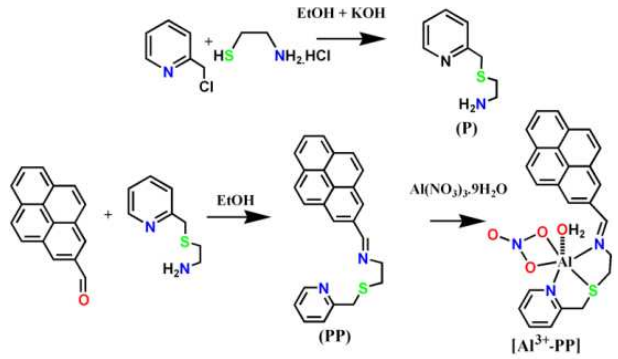

Scheme 1

The UV-Vis spectrum of sensor **PP** was recorded in a MeOH-H_2O (9:1, v/v) at pH 7.2 (1mM HEPES buffer)which displayed well-defined bands at 390, 360, 344, 285 and 275 nm typical of pyrene moiety. On gradual addition of Al^{3+} there is an increase in absorbance at all these wavelengths along with the development of a new band at 440 nm (**Fig. 1**).This indicates a complexation between **PP** and Al^{3+}. However, no such significant change in the absorption spectrum of **PP** was observed with other tested metal cations.

The composition of complex formed by the reaction between **PP** and Al^{3+} was determinedby absorption titration in MeOH-H_2O (9:1, v/v) at pH 7.2 (1mM HEPES buffer) (**Fig. 1**). The OD (optical density) at 440 nm increases gradually with the increase in concentration of Al^{3+}up to a mole ratio **PP**:Al^{3+} = 1:1 (**Fig. 1A**) and then becomes saturated. When we plot $[(A_{max}-A_o)/(A-A_0)]$ vs. $1/[Al^{3+}]$ the slope of such plot gives a value of K_d = (1.94 ± 0.04) x 10^{-4} M (**Fig. 1B**) and n = 1 indicating 1:1 binding between **PP** and Al^{3+}. Job's method was further employed to determine the composition of the complex that also indicates a 1:1 complexation (**Fig. 1C**). The probe acts as a naked eye colorimetric sensor for Al^{3+} with the change in colour from colorless to greenish yellow **(Fig. S8).**

In the absence of Al^{3+}, **PP** isvery weakly fluorescent compared to that of pyrene due to photo-induced electron transfer (PET) from the metal binding site (azomethyne-N) to the fluorescent pyrene unit.The *cis-trans* isomerisation around the C=N bond of azomethyne group may be neglected by considering the positive dihedral angles (C=N–C–C) which were found to be 125.878 for PP and 117.442 for PP+Al^{3+},[31] indicating the existence of sole *cis*-isomer in both cases (vide supra). The fluorescence enhancement observed for compound **PP** in the presence of Al^{3+} ions was attributed to the chelation enhanced fluorescence (CHEF) effects arising through coordination of azomethine-N along with pyridine-N and S atoms to the metal ion, as a result PET effect is efficiently blocked.

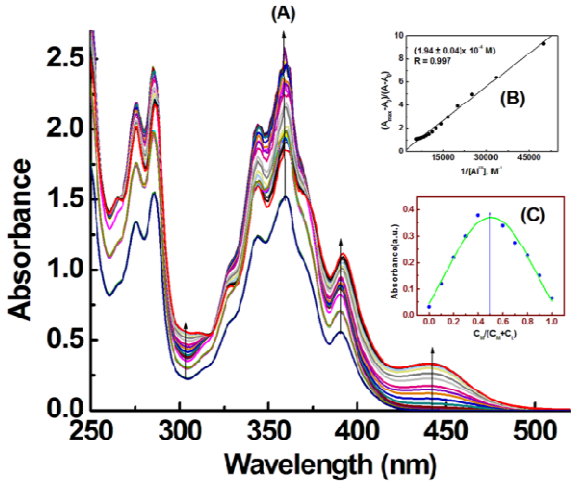

Fig. 1(A) Absorption titration of **PP** (20μM) with Al^{3+} in MeOH-H_2O (9:1,v/v, pH 7.2, HEPES buffer). Inset shows **(B)** Benesi-Hilderbrand plot.**(C)**Job's Plot.

Pyrene seems to be an interesting fluorophore displaying a change in excimer–monomer emission intensities [32,33,34] due to the formation of self-assembled pyrene-conjugate. In our case we performed DLS (Dynamic Light Scattering) studies to check such possibilities. It was interesting to note that excimer formation takes place through intermolecular π···π stacking between pyrene moieties both in absence and presence of Al^{3+}. In the DLS spectrum of free ligand the peak corresponding to diameter 1.14 nm may be due to PP monomer while peak corresponding to diameter ~232 nm is due to excimer. However, such aggregation is much favoured in presence of Al^{3+} as indicated by the increase in particle size in presence of metal ion (**Fig. S9 and Table S1**). Here PP-Al^{3+} monomer size is 5.40 nm while the diameter of excimer is 359 nm.

The emission spectra of **PP** and its fluorescence titration with Al^{3+} were recorded in MeOH-H_2O (9:1) at pH 7.2, 1.0 mM HEPES buffer (**Fig. 2**). The binding between the free probe **PP** and Al^{3+} leads to chelation enhanced fluorescence (CHEF) effect causing fluorescence enhancement (FE) at 506 nm due to blocking PET effect. A plot of F.I. vs. $[Al^{3+}]$ gives a non-linear curve with decreasing slope at higher concentration of Al^{3+}.

A Benesi-Hiderband plot of $[F_{max}-F_o)/(F-F_o)]$ vs. $1/[Al^{3+}]$ gives straight line with slope K_d =(2.55 ± 0.10) x 10^{-4} M with R^2 = 0.99, indicating 1:1 complexation. It is to be mentioned here that there is an excellent agreement between the K_d values obtained from two spectroscopic titrations indicating the self-consistency of our results. The LOD of Al^{3+} calculated by using 3σ method was found to be 15nM (**Fig. S12**).

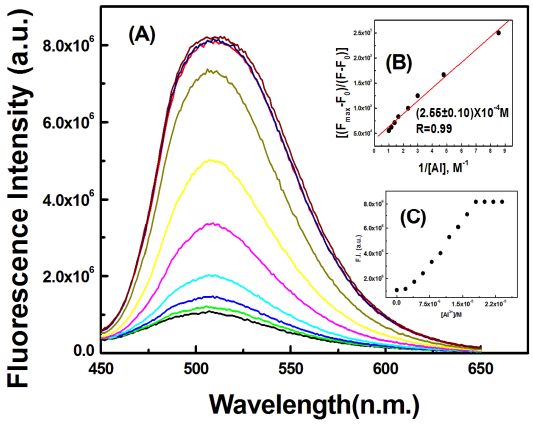

Fig.2 (A) Fluorescence titration of **PP** (20 μM) in MeOH-H_2O (9:1,v/v, pH 7.2, HEPES buffer) by the gradual addition Al^{3+} with λ_{ex} = 440 nm, λ_{em} = 506 nm Inset. **(B)** Benesi-Hilderbrand Plot. **(C)** Plot of F.I. vs. [Al^{3+}].

A K_d value of (2.55 ± 0.10) x 10^{-4} M unambiguously demonstrates a moderate binding of **PP** towards Al^{3+}.The stoichiometry of Al^{3+} complex with **PP** as delineated by UV-VIS and fluorescence titrations was further confirmed by ESI-MS^+ (m/z) mass spectrometry $[Al(\mathbf{PP})(NO_3^-)(H_2O)]^{2+}$ (m/z = 245.1001) (**Fig. 3**) and Job's method. Al^{3+} detection was not perturbed by biologically abundant Na^+, K^+, Ca^{2+} etc metal ions. Several transition metal ions, namely Cr^{3+}, Mn^{2+}, Fe^{2+}, Fe^{3+}, Co^{2+}, Ni^{2+}, Cu^{2+}, and heavy metal ions like Cd^{2+}, Pb^{2+}, and Hg^{2+}, also cause no interference (**Fig. 4**). The sensor was found to bind Al^{3+} reversibly as tested by reacting with excess H_2EDTA^{2-} under both intra- and extracellular conditions (**Fig. S13and Fig. 10**).

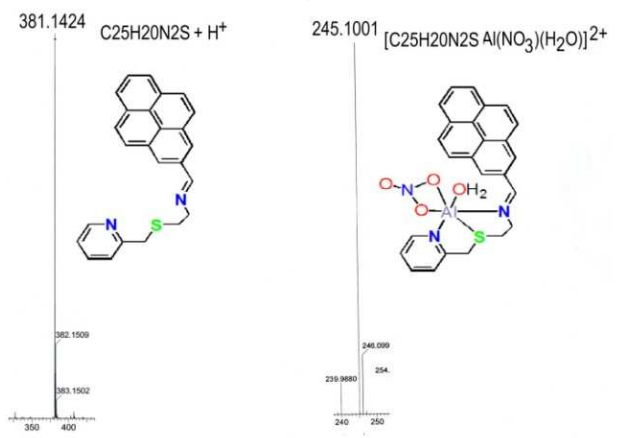

Fig.3HRMS spectra of (a) PP and Al^{3+}–PP complex in the positive mode.

In order to support the binding of Al^{3+} with the receptor **PP**, the ^1H NMR titration was performed in DMSO-d_6 (**Fig. 5**). The ^1H NMR spectrum of PP contains signals for the HC=N (azomethine, H) at 9.27 ppm and pyridine protons (a, b, c, and d) appear at 7.40(d), 7.71(t), 7.22 (t) and 8.99 (d) ppm, respectively. The pyrene protons appear in the region 8.05-8.48 ppm. The chemical shifts for other protons appear in the usual positions. Addition of 1.2 equivalent of $Al(NO_3)_3{\cdot}9H_2O$ leads to a down field shift of the azomethine proton (9.32 ppm) and d proton (9.29 ppm) on the pyridine ring. All other protons remain almost invariant in presence of Al^{3+} ion. This clearly indicates the involvement of the azomethine N and pyridine N atoms in bonding with Al^{3+}.

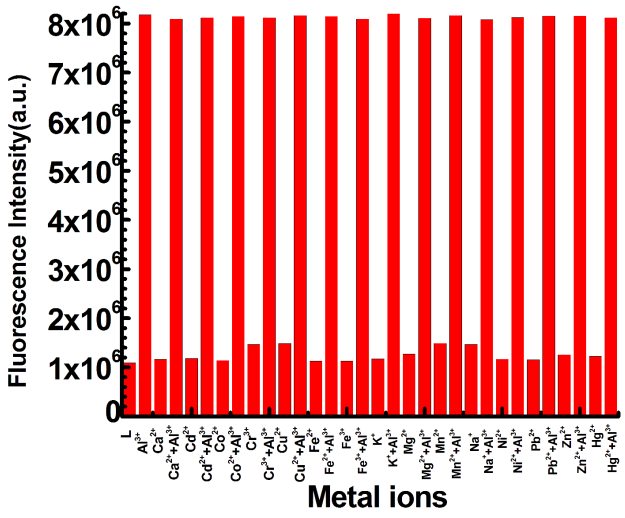

Fig.4 Bar chart illustrating fluorescence response of PP at 506 nm towards different cations in MeOH-H_2O (9:1, v/v) at pH 7.2. Conditions: PP = 20 μM, M^{n+} = 100 μM; where, M^{n+} = Al^{3+}, Ca^{2+}, Cd^{2+}, Co^{2+}, Cr^{3+}, Cu^{2+},Fe^{2+},Fe^{3+}, K^+, Mg^{2+}, Mn^{2+}, Na^+, Pb^{2+}, Zn^{2+}, Hg^{2+}.

Geometry optimization and electronic structure

The optimized geometry of **PP** and its Al^{3+}**-PP** complex is shown in **Fig. 6.** The composition of the complex as [[Al(**PP**)$(NO_3)(H_2O)$] is based on HRMS studies which displayed the presence of one NO_3^- and one water molecules in the molecular fragment. Both PP and Al^{3+}**-PP** complex has *C*1 point group. The important optimized geometrical parameters of the complex are listed in **Table 1**. The hexa-coordinated

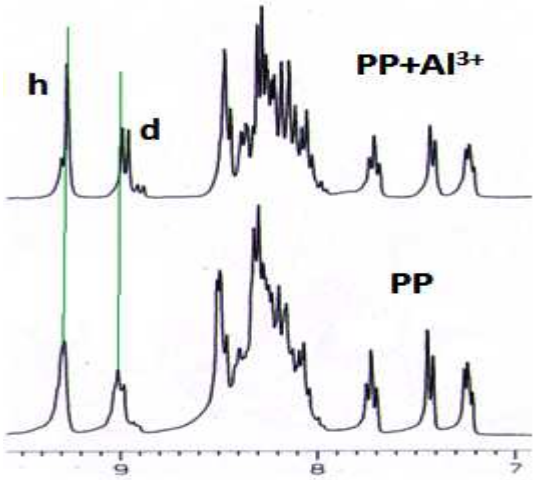

Fig. 5^1H NMR spectra of PP and Al^{3+}–PP complex in DMSO- d_6 on 300 MHz Bruker Instrument.

Table 1 Selected optimized geometrical parameters for 1 in the ground state.

Bond Lengths (Å)			
Al-N1	2.02	Al-O1	2.06
Al-N2	2.05	Al-O2	1.99
Al-S	2.52	Al-O3w	1.95
Bond Angles (°)			
N1-Al-S	85.53	N2-Al-O2	95.93
N2-Al-S	78.5	N2-Al-O3w	83.82
N2-Al-Ol	102.31	N1-Al-O1	93.89
O1-Al-S	84.29	N1-Al-O2	107.05
O3w-Al-S	119.77	N2-Al-O3w	88.61
O1-Al-O2	65.73	O2-Al-O3w	90.65

Table 2 Change in bond lengths for 1 compared to free L in the ground state calculated at B3LYP Levels

Bond Lengths (Å)		
	Free ligand (L)	Complex 1
N1-C1	1.284	1.327
N1-C2	1.464	1.504
S-C3	1.903	1.908
S-C4	1.916	1.906
N2-C5	1.355	1.374
N2-C6	1.351	1.365

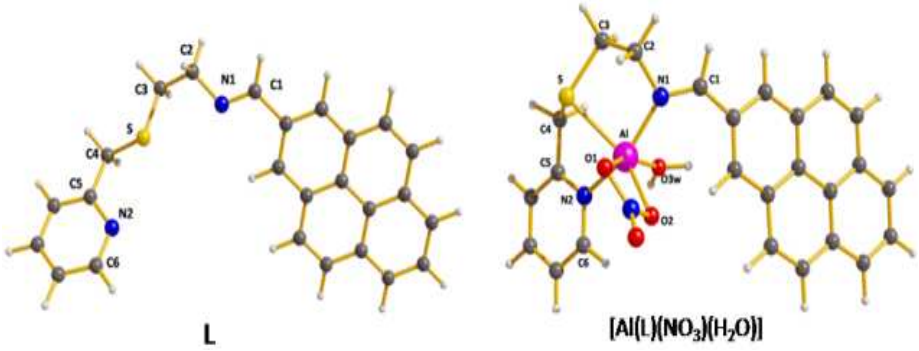

Fig. 6 Optimized geometry of ligand (**PP**) and $[Al(\mathbf{PP})(NO_3)(H_2O)]^{2+}$.

metal centre possesses a distorted octahedral geometry. The calculated Al–N and Al–O bond distances fall in the range 2.020-2.054 and 1.954-2.060 Å, respectively. On complexation, some C–N and C–S bond distances are changed with respect to that in free ligand. **Table 2** describes the change in bond lengths in Al^{3+}**-PP** compared to free ligand **PP**.

In case of **PP** in the ground state, the electron density resides mainly on HOMO-2, HOMO, LUMO and LUMO+1 molecular orbitals of the pyrene moiety while in HOMO-1 and LUMO+3 molecular orbitals a considerable contribution comes from cystemine moiety along with the contribution from pyridyl moiety with an energy gap between HOMO and LUMO of 3.872 eV (**Fig. 7**). In case of Al^{3+}**-PP** complex all the HOMO-2, HOMO-1 and HOMO molecular orbitals are mainly originating from ligand π and π* orbitals while LUMO+1 and LUMO+3 molecular orbitals arise from metal d orbitals along with ligand π orbitals with HOMO–LUMO energy gap of 1.82 eV. These compositions are useful in understanding the nature of transition as well as the absorption spectra of both the ligand and complex.

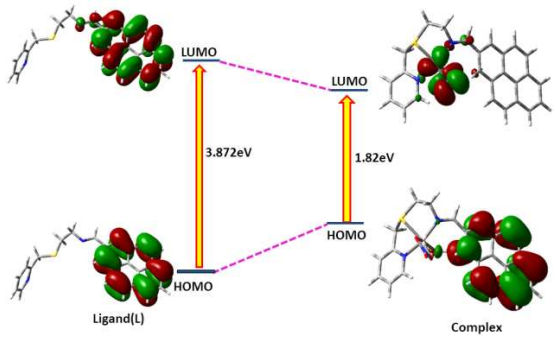

Fig. 7 Frontier molecular orbital of **PP** and $[Al(\mathbf{PP})(NO_3)(H_2O)]^{2+}$

The ligand shows four absorption bands at 343, 286/275, 263/260 and 243/233 nm in a methanolic solution at room temperature and have ILCT character due to the presence of pyrene moiety. These bands are assigned to $S_0 \rightarrow S_2$, $S_0 \rightarrow S_7$, $S_0 \rightarrow S_{11}$ and $S_0 \rightarrow S_{17}$ electronic transitions, respectively (**Fig. 8**). The absorption energies along with their oscillator strengths are given in **Table S2**. The Al^{3+}-**PP** complex shows three absorption bands at 390, 360 and 343 nm (**Fig. 9)** in methanol at room temperature and the corresponding calculated absorption bands are located at 394, 357 and 334 nm which are in excellent agreement with experimental results (**Table S3 and Table 3**). These three absorption bands can be assigned to the $S_0 \rightarrow S_6$, $S_0 \rightarrow S_8$ and $S_0 \rightarrow S_{11}$ transitions, respectively originating from an admixture of MLCT and ILCT transitions (**Table S2**).

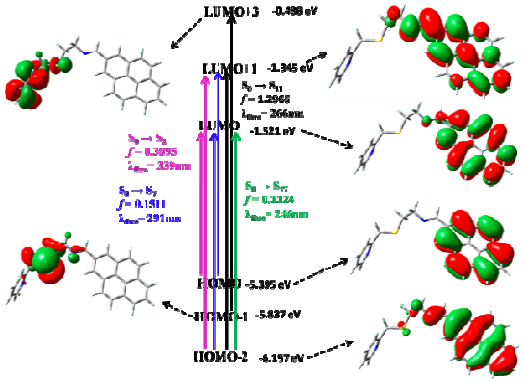

Fig. 8 Frontier molecular orbitals involved in the UV-Vis absorption of ligand (**PP**).

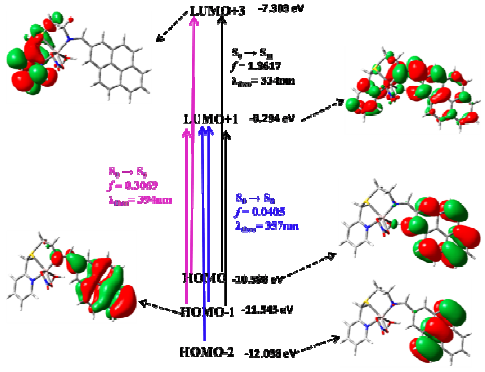

Fig. 9 Frontier molecular orbitals involved in the UV-Vis absorption of $[Al(\mathbf{PP})(NO_3)(H_2O)]^{2+}$.

Table 3 Thecomparable calculated optical transitionswith Experimental UV/Vis values for the ligand (**PP**) and complex $[Al(\mathbf{PP})(NO_3)(H_2O)]^{2+}$.

Ligand and complex 1	Experimental [λ_{exp} (nm)]	Theoretical [λ_{theo} (nm)]	Electronic transition
Ligand	343	339	$S_0 \rightarrow S_2$
Ligand	286/275	291	$S_0 \rightarrow S_7$
Ligand	263/260	266	$S_0 \rightarrow S_{11}$
Ligand	243/233	246	$S_0 \rightarrow S_{17}$
complex 1	390	394	$S_0 \rightarrow S_6$
complex 1	360	357	$S_0 \rightarrow S_8$
complex 1	343	334	$S_0 \rightarrow S_{11}$

The intracellular imaging behaviours of **PP** on HepG2 cells with the aid of fluorescence microscopy displayed weak intracellular fluorescence when treated with 10 μM **PP** (**Fig. 10**)**.** This weak fluorescence response towards the probe was due to the presence of intracellular Al^{3+}, though may be in a very low concentration; but very low detection limit (semi-ppb level, *vide infra*) of this probe for Al^{3+} enablesus to visualize the presence of intracellular Al^{3+}. Fluorescence images of HepG2 cells were taken separately for another set of experiment where cells incubated with 10 μM PP+10μM Al^{3+} for 30 min where bright fluorescence was observed. Similarly, in another set of experiment, cells were incubated with 10μM PP+10μM Al^{3+} for 30 min followed by addition of 100μM H_2EDTA^{2-} for another 30 min and fluorescence images were taken. In this case, HepG2 cells showed almost complete quenching of fluorescence due to removal of Al^{3+} from the PP+ Al^{3+} complex by H_2EDTA^{2-} which manifests a reversible binding of PP towards Al^{3+}, satisfying one of the crucial requirements for *in-vivo*monitoring of a chemical species.

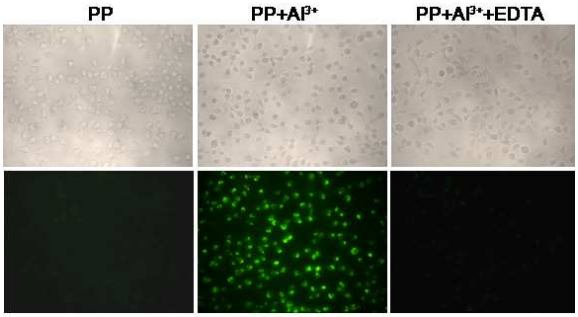

Fig. 10 The phase contrast and fluorescence images of HepG2 cells were capture after incubated with PP, PP+Al^{3+}, for 30 min at 37°C and followed by addition of 100μM H_2EDTA^{2-} after cells being pre incubated with PP+Al^{3+} for 30 min at 37°C.

For convenient biological application of this probe under physiological conditions it is necessary to verify its pH-stability. There is no obvious fluorescence emission of PP between pH 4 and 12, which suggests that PP is stable over this wide range of pH and can work well under physiological conditions (**Fig. 11**).

However, in presence of selective guest like Al^{3+} ion it fluoresces effectively in the range pH 4.0-8.0 with almost constant intensity which clearly indicates the compatibility of the probe for biological applications under physiological conditions. At pH ≥ 8.0 there is gradual decrease in FI may be due to the formation of $Al(OH)_2^+$ $Al(OH)_3$ and $Al(OH)_4^-$ depending on pH of the medium.

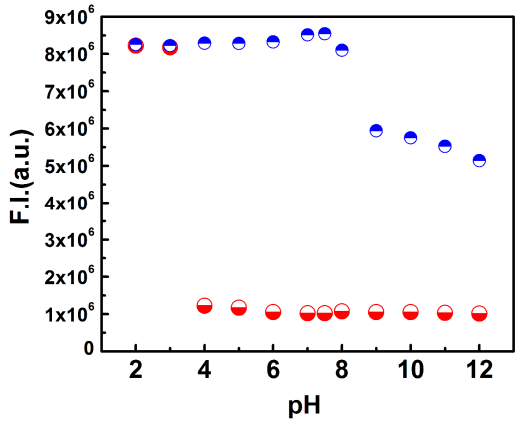

Fig. 11 pH study of PP and corresponding Al^{3+} complex

A comparison of our probe, with the previously reported pyrene based analogous systems is shown in the Chart 1. A quick inspection of these studies reveal that all these are turn-on sensor towards different metal ions with moderate LOD values.

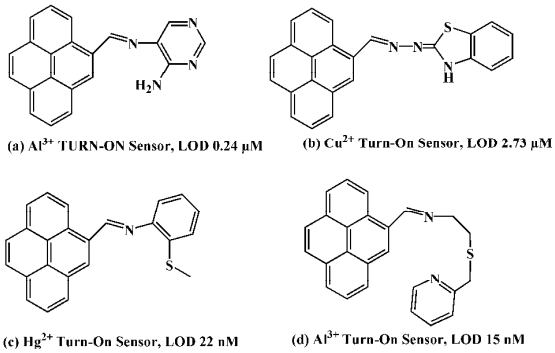

Chart 1. Comparison of some previously reported systems (a,b,c) with our probe (d).

Conclusion

In summary, we have synthesized a novel pyrene based N_2S donor probe for selective recognition of Al^{3+}, in presence of large number of background metal ions, which was found to undergo 1:1 complexation in MeOH-H_2O (9:1, v/v, pH 7.2, HEPES buffer). The probe itself is very weakly fluorescent due to combined PET effect arising out of the transfer of electron from azomethine-N to the pyrine moiety in the excited state. It becomes fluorescent only in presence of Al^{3+} which causes PET blocking through selective coordination to the Al^{3+}. The complexation of PP to Al^{3+} was confirmed by ^1H NMR and ESI-MS^+ studies and further strengthened by DFT calculations on both the free ligand and its Al^{3+} complex. The UV-Vis and Fluorescence titrations help us to delineate K_d values (1.94 x 10^{-4} M and 2.55 x 10^{-4} M, respectively) which are in excellent agreement manifesting the self-consistency of our results. The reversible binding of Al^{3+} to PP was confirmed by reacting with excess H_2EDTA^{2-} both in extra- and intracellular conditions.

Experimental

Materials and Methods.

The starting materials, such as, cystamine hydrochloride (Sigma Aldrich), 2-chloromethyl pyridine (Sigma Aldrich) were used for the preparation of amine and then used to condense with pyrene carboxyaldehyde (Sigma Aldrich) for the preparation of ligand PP. $Al(NO_3)_3.9H_2O$ (Sigma Aldrich) was used to prepare Al^{3+} complex. Solvents like MeOH, MeCN etc (Merck, India) were of reagent grade.

Physical Measurements

Elemental analyses were carried out using a Perkin–Elmer 240 elemental analyzer. Infrared spectra (400–4000 cm^{-1}) were recorded from KBr pellets on a Nickolet Magna IR 750 series-II FTIR spectrophotometers. ^1H-NMR was recorded in $CDCl_3$ and DMSO-d_6 on a Bruker 300 MHz NMR spectrometer using tetramethylsilane (δ = 0) as an internal standard. UV-Vis spectra were recorded on an Agilent diode-array spectrophotometer (Model, Agilent 8453), Steady-state Fluorescence were recorded on a PTI spectrofluorimeter (Model QM-40.), ESI-MS^+ (m/z) of the amine, ligand **(PP)** and Al^{3+}-**PP** complex were recorded on a HRMS spectrometer (Model: QTOF Micro YA263).

Syntheses

Preparation of(2-(Pyridin-2'-ylmethylsulfanyl) ethanamine) (P)

2-Aminoethanethiol hydrochloride (12.2 mmol) and the 2-(chloromethyl)pyridine hydrochloride (6.1 mmol) were added to a solution of NaOH (24.4 mmol) in EtOH (20 mL) in ice bath. The reaction mixture was stirred for 30 min before the ice bath was removed and then the mixture was stirred at an ambient temperature for 2.5 h. The EtOH was removed under reduced pressure and water (25 mL) was added to the resulting residue. The aqueous solution was extracted with CH_2Cl_2 (3 x 25 mL) and the combined organic layer was washed with brine (20 mL), dried with K_2CO_3, filtered and solvent was removed in vacuo to afford a crude oil. It was further purified by column chromatography (silica, CH_2Cl_2/MeOH/NH_3 =9/2/0.04) to give 1.78 g as yellow liquid in 89% yield. Anal. Calcd for $C_8H_{12}N_2S$: C, 57.11; H, 7.19; N, 16.65. Found: C, 57.55; H, 7.33; N, 16.07.^1H NMR (300 MHz, $CDCl_3$) (δ, ppm): 2.01(b,2H, NH2),2.77(t, 2H, CH2), 2.55(t, 2H,CH2), 3.77(s,2H,CH2), 7.30(d, 1H, ArH), 7.58(t,1H, ArH), 7.11(t,1H,ArH), 8.46(d,1H,ArH)(**Fig. S1**). Mass spectrum: m/z= 169.1076(**P +** H^+), 191.0693 (**P +** Na^+)(**Fig. S4**).

Pyrene-2-(Pyridin-2-ylmethylsulfanyl)-ethylamine (PP)

Pyrenecarboxaldehyde (0.460 g, 2 mmol) was dissolved in 25 mL MeOH. To this solution was added P (0.336 g, 2 mmol) drop wise

and stirred at room temparature for 2h and then the reaction mixture was filtered out and evaporated to dryness in rota-evaporator. After that liquid product was collected and purified by column chromatography. (neutral allumina, CH_2Cl_2/MeOH =8/2) (yield, 80.34%). Anal. Calcd for $C_{25}H_{20}N_2S$: C, 78.91; H, 5.30; N, 7.36. Found: C, 78.55; H, 5.53; N, 7.24. ^{1}H-NMR (in DMSO-d_6) (δ, ppm): 2.88(t, 2H, CH2), 3.94(4H,CH2, CH2), 7.40(d, 1H, ArH), 7.71(t,1H, ArH), 7.22 (t,1H,ArH), 8.99(d,1H,ArH) , 9.27(s, 1H, azomethane) and 8.05-8.48 (9H,pyrene protons) (**Fig. S2**). ESI-MS$^+$ (m/z): 381.1424 (**PP**+H$^+$) **(Fig. S5)**.

Synthesis of Complex

To a solution of **PP** (0.76 g, 2 mmol) in 30 ml MeOH was added $Al(NO_3)_3.9H_2O$ (0.75 g, 2 mmol) in 20 ml MeOH drop wise with continuous stirring. After 1 hour the solution was filtered and kept aside undisturbed. After one day crystalline complex was precipitated out. It was collected by filtration, washed several times with MeOH and dried in air. It was recrystallized from methanol. Several trials to grow single crystals were failed. Elemental analysis for $C_{25}H_{22}N_3O_4S$: calculated: C, 61.59; H, 4.55; N, 8.62; Found: C, 61.55; H, 4.53; N, 8.74 2.90(t, 2H, CH2), 3.96(4H,CH2, CH2), 7.43(d, 1H, ArH), 7.71(t,1H, ArH), 7.24 (t,1H,ArH), 9.28(d,1H,ArH) , 9.32(s, 1H, azomethane) and 8.06-8.97(9H,pyrene protons) (**Fig. S3**). ESI-MS$^+$ (m/z): 245.1001 ([Al(**PP**)(NO_3^-)(H_2O)]$^{2+}$) (**Fig. S6**).

Computational details

Ground state electronic structure calculations in methanol solution of both the ligand and complex have been carried out using DFT method[35] associated with the conductor-like polarizable continuum model (CPCM).[36] Becke's hybrid function[37] with the Lee-Yang-Parr (LYP) correlation function[38]was used throughout the study. The geometry of the ligand and complex were fully optimized without any symmetry constraints. On the basis of the optimized ground state geometry, the absorption spectral properties **PP** and Al^{3+}-**PP** in methanol were calculated by time-dependent density functional theory (TDDFT)[39] associated with the conductor-like polarizable continuum model (CPCM).[36] We have computed the lowest 40 singlet– singlet transitions and the presence of electronic correlation in the TDDFT (B3LYP) method[40] enables to get accurate electronic excitation energies.

For H atoms we used 6-31G basis set; for C, N, O and Al atoms we employed 6-31G and for S atom we adopt 6-31 + G(d,p) basis sets for the optimization of the ground state. The calculated electronic density plots for frontier molecular orbitals were prepared by using Gauss View 5.1 software. All the calculations were performed with the Gaussian 09W software package.[41] Gauss Sum 2.1 program[42]was used to calculate the molecular orbital contributions from groups or atoms.

Cell culture

HepG2 cell line, Human hepatocellular liver carcinoma cells, were procured from National Center for Cell Science, Pune, India, and used throughout the study. Cells were cultured in DMEM (Gibco BRL) supplemented with 10% FBS (Gibco BRL), and a 1% antibiotic mixture containing Penicillin, Streptomycin and Gentamicin (Gibco BRL) at 37°C in a humidified incubator with 5% CO_2 and cells were grown to 60-80% confluence, harvested with 0.025% trypsin (Gibco BRL) and 0.52 mM H_2EDTA^{2-} (Gibco BRL) in phosphate-buffered saline (PBS), plated at the desired cell concentration and allowed to re-equilibrate for 24 h before any treatment.

Cell Cytotoxicity Assay

To test the cytotoxicity of PP assay was performed as per the procedure described earlier.[43]
After treatment with PP at different doses of 1, 10, 20, 50 and 100 μM, respectively, for 12 h, 10 μl of MTT solution (10 mg/ml PBS) was added to each well of a 96-well culture plate and again incubated continuously at 37ºC for a period of 3 h. All media were removed from wells and 100 μl acidic isopropyl alcohol was added into each well. The intracellular formazan crystals (blue-violet) formed were solubilized with 0.04 N acidic isopropyl alcohol and absorbance of the solution was measured at 595 nm with a microplate reader (Model: THERMO MULTI SCAN EX). The cell viability was expressed as the optical density ratio of the treatment to control. Values were expressed as mean ± standard errors of three independent experiments. The cell cytotoxicity was calculated as % cell cytotoxicity = 100% - % cell viability(**Fig. S14**).

Cell Imaging Study

HepG2 Cells were incubated with 10 μM PP [the stock solution (1 mM) was prepared by dissolving PP to the mixed solvent (DMSO: water = 1:9 (v/v)] in the culture medium, allowed to incubate for 30 min at 37 °C. After incubation, cells were washed twice with phosphate-buffered saline (PBS). Bright field and fluorescence images of HepG2 cells were taken by a fluorescence microscope (Leica DM3000, Germany) with an objective lens of 40X magnification. Fluorescence images of HepG2 cells were taken separately from another set of experiment where cells incubated with 10μM PP+10μM Al^{3+} for 30 min. Similarly, in another set of experiment, cells were incubated with 10μM PP+10μM Al^{3+} for 30 min followed by addition of 100μM H_2EDTA^{2-} for another 30 min and fluorescence images were taken. HepG2 cells showed almost complete quenching of fluorescence due to removal of Al^{3+} from the complex.

Acknowledgement

Financial support from DST (Ref. SR/S1/IC-20/2012) New Delhi is gratefully acknowledged.

References

1 K. Soroka, R. S. Vithanage, D. A. Phillips, B. Walker and P. K. Dasgupta, *Anal. Chem*. 1987, **59,** 629.
2 S. H. Kim, H. S. Choi, J. Kim, S. J. Lee, D. T. Quang and J. S. Kim, *Org. Lett.* 2010, **12**, 560.
3 M. Dong, Y.M. Dong, T.H. Ma, Y.W. Wang and Y. Peng, *Inorg.Chim.Acta* 2012, **381**, 137.
4 T. Han, X. Feng, B. Tong, J. Shi, L. Chen, J. Zhic and Y. Dong, *Chem. Commun*. 2012, **48**, 416.
5 X. Sun, Y.W. Wang and Y. Peng, *Org. Lett.* 2012, **14**, 3420.
6 K. K. Upadhyay and A. Kumar, *Org. Biomol. Chem.* 2010, **8**,

4892.
7 J. Y. Jung, S. J. Han, J. Chun, C. Lee and J. Yoon, *Dyes Pigm.* 2012, **94**, 423.
8 J. R. Lakowicz, Topics in Fluorescence Spectroscopy: Probe Design and Chemical Sensing, Kluwer Academic Publishers, New York, 2002, 4.
9 M. G. Soni, S. M. White, W. G. Flamm and G. A. Burdock, *Regul. Toxicol.Pharmacol.* 2001, **33**, 66.
10 (a) T. P. Flaten and M. Odegard, *Food Chem. Toxicol.* 1988, **26**, 959; (b) J. Ren and H. Tian, *Sensors*, 2007, **7**, 3166; (c) R. A. Yokel, *Neurotoxicology*, 2000, **21**, 813.
11 E. Delhaize and P. R. Ryan, Plant Physiol. 1995, **107**, 31.
12 (a) J. Barcelo and C. Poschenrieder, *Environ. Exp. Bot* 2002, **48**, 75; (b) B. Valeur and I. Leray, *Coord. Chem. Rev.* 2000, **205**, 3; (c) Z. Krejpcio and R. W. P. Wojciak, *J. Environ. Studies* 2002, **11**, 251.
13 (a) G. D. Fasman, *Coord. Chem. Rev*. 1996, 149, 125; (b) P. Nayak, *Environ. Res.* 2002, **89**, 111; (c) C. S. Cronan, W. J. Walker and P. R. Bloom, *Nature* 1986, **324**, 140; (d) G. Berthon, *Coord. Chem. Rev*. 2002, **228**, 319; (e) D. R. Burwen, S. M. Olsen, L. A. Bland, M. J. Arduino, M. H. Reid and W. R. Jarvis, *Kidney Int.* 1995, **48**, 469.
14 (a) O. Y. Nadzhafova, S.V. Lagodzinskaya and V. V. Sukhan, *J. Anal. Chem.* 2001, **561**, 78; (b) M.J. Ahmed and J. Hossan, *Talanta.* 1995, **42,** 1135; (c) M. Ahmad and R. Narayanaswamy, *Sensors Actuators B Chem*. 2002, **81,** 259.
15 R. Flarend and D. Elmore, Aluminum-26 as a biological tracer using accelerator mass spectrometry, in: P. Zatta, A.C. Alfrey (Eds.), Aluminum in Infant's Health and Nutrition, 5 World Scientific, Singapore, 1997, 16.
16 J. L. McDonald-Stephens and G. Taylor, *Plant Physiol.* 1995, **145,** 327.
17 R.F. Fleming and R.M. Lindstrom, *J. Radioanal. Nucl.Chem.* 1987, **113,** 35.
18 J.C. Rouchaud, N. Boisseau and M. Fedoroff, *J. Radioanal. Nucl. Chem. Lett.* 1993, **175,** 25.
19 B. Rietz, K. Heydorn and G. Pritzl, *J. Radioanal. Nucl.Chem.* 1997, **216,** 113.
20 M.A. Lovell, *Ann. Neurol*. 1993, **33,** 36.
21 S. Knežević, R. Milačič and M. Veber, *J. Anal.Chem*. 1998, **362,**162.
22 (a) J. W. Zhu, Y. Qin and Y. H Zhang, *Anal. Chem*. 2010, **82**, 436; (b) T. Y. Han, X. Feng, B. Tong, J. B. Shi, L. Chen, J. G. Zhi and Y. P. Dong, *Chem. Commun*. 2012, **48**, 416; (c) S. Anbu, S. Shanmugaraju, R.Ravishankaran, A. A. Karande and P. S. Mukherjee, *Dalton Trans*. 2012, **41**, 13330.
23 (a) U. E. Spichiger-Keller, Chemical Sensors and Biosensors for Medical and Biological Applications, Wiley-VCH, Weinheim, Germany, 1998; (b) V. Amendola, L. Fabbrizzi, F. Forti, M. Licchelli, C. Mangano, P. Pallavicini, A. Poggi, D. Sacchi and A. Taglieti, *Coord. Chem. Rev*. 2006, **250**, 273; (c) K. Rurack and U. Resch-Genger,*Chem. Soc. Rev.* 2002, **31**, 116; (d) P. T. Srinivasan, T. Viraraghavan and K. S. Subramanian, Water SA, 1999,**25**, 47.
24 (a)T. Mistri, R. Alam,R. Bhowmick, S.K. Mandal, M. Dolai, A.R. Khudabukhsh and M. Ali, *Analyst,* **DOI:** 10.1039/C3AN02255B; (b) M. Arduini and P. Tecilla, Chem.*Commun.,* 2003, **25**, 1606; (c) J. S. Kim, J. Vicens, *Chem. Commun*., 2009, **45**,4791; (d) S. Kim, J. Y. Noh, K. Y. Kim, J. H. Kim, H. K. Kang, S. W. Nam, S. H. Kim, S. Park, C. Kim and J. Kim, *Inorg. Chem.*, 2012, **51**, 3597; (e) F. K. Hau, X. M. He, W. H. Lam and V. W. Yam, *Chem. Commun.*, 2011, **47**, 8778; (f) Y. Lu, S. S. Huang, Y. Y. Liu, S. He, L. C.Zhao and X. S. Zeng, *Org. Lett*., 2011, **13**, 5274; (g) D. Maity and T. Govindaraju, *Chem. Commun.,* 2010, 46, 4499; (h) Y. Dong, J. F. Li, X. X. Jiang, F. Y. Song, Y. X. Cheng and C. J. Zhu, Org. Lett., 2011, **13**, 2252; (i) L. Wang,W. Qin, X. Tang, W. Dou, W. Liu, Q. Teng and X. Yao, *Org. Biomol. Chem.,* 2010, **8**, 3751; (j) K. K. Upadhyay and A. Kumar, *Org. Biomol. Chem.,* 2010, **8**, 4892; (k) A. Sahana, A. Banerjee, S. Das, S. Lohar, D. Karak, B. Sarkar, S. K. Mukhopadhyay A. K. Mukherjee and D. Das,*Org. Biomol. Chem.,* 2011, **9**, 5523.
25 (a) W-H Ding, W.Cao, X-J. Zheng, D-C.Fang, W-T Wong, and L-P Jin; *Inorg.Chem*. 2013, **52**, 7320 (b) D. Maity and T. Govindaraju, *Inorg.Chem*. 2010, **49**, 7229; (c) S. Sinha, R. R. Koner, S. Kumar, J.Mathew, Monisha, P. V., I. Kazia and S. Ghosh, *RSC Adv*. 2013, **3**, 345.
26 a) S. Kim, J. Y. Noh, K. Y. Kim, J. H. Kim, H. K. Kang, S-W. Nam, S. H. Kim, S. Park, C. Kim and J. Kim; *Inorg.Chem.* 2012, **51**, 3597; b) C-H.Chen, D-J.Liao, C.-F.Wan and A-T.Wu; *Analyst* 2013, **138**, 2527.
27 (a) S. M. Z. Al-Kindy, F. E. O. Suliman and A. E. Pillay,*Instrum. Sci. Technol*. 2006, **34**, 619; (b) J. L. Ren, J. Zhang, J. Q. Luo, X. K. Pei and Z. Xi Jiang, *Analyst* 2001, **126**, 698; (c) S. M. Ng and R. Narayanaswamy, *Anal. Bioanal.Chem.* 2006, **386**, 1235; (d) Y.-W.Wang, M.-X.Yu, Y.-H.Yu, Z.-P.Bai, Z. Shen, F.-Y.Li and X.-Z.You, *Tetrahedron Lett.* 2009, **50**, 6169.
28 Y. Lu, S. Huang, Y. Liu, S. He, L. Zhao, and X. Zeng, *Org. Lett.* 2011,13, 5274.
29 J. Liang and J. W. Canary, *Angew. Chem. Int. Ed.,* 2010, **49**, 7710.
30 S. J. Mountford , E. M. Campi , A. J. Robinson, M.T.W. Hearn, Tetrahedron 2011, **67**, 471.
31 G. Sivaraman, T. Anand and D. Chellappa, RSC Advances, 2012, **2**, 10605.
32 (a) F. M. Winnick, Chem. Rev. 1993, **93**, 587; (b) S. Karuppannan and J. C. Chambron, Chem.Asian J. 2011, **6** ,964; (c) A. E. C. Redpath and M. A. Winnik, J. Am. Chem. Soc. 1982, **104**, 5604; (d) M. A. Winnik and S. M. Bystryak, Z. Liu, J. Siddiqui, Macromolecules 1998, **31**, 6855.
33 (a) S. Nishizawa, Y. Kato and N. Teramae, J. Am. Chem. Soc.1999, **121**, 9463; (b) D. Sahoo, V. Narayanaswami, C. M. Kay and R. O. Ryan, Biochemistry 2000, **39,** 6594.
34 G. Sivaraman, T. Anand and D. Chellappa, Anal. Methods, 2014, **6**, 2343.
35 R. G. Parr, W. Yang, Density Functional Theory of Atoms and Molecules, Oxford University Press, Oxford, 1989.
36 (a) V. Barone and M. Cossi, J. Phys. Chem. A 1998, **102 ,**1995; (b) M. Cossi and V. Barone, J. Chem. Phys. 2001, **115**, 4708; (c) M. Cossi, N. Rega, G. Scalmani, V. Barone and J. Comp. Chem. 2003, **24**,669.
37 A. D. Becke, J. Chem. Phys. 1993, **98** ,5648.
38 C. Lee, W. Yang and R. G. Parr, Phys. Rev. B 1998, **37 ,**785.
39 (a) M. E. Casida, C. Jamoroski, K. C. Casida and D. R. Salahub, J. Chem. Phys. 1998, **108**, 4439; (b) R. E. Stratmann, G. E. Scuseria and M. J. Frisch, J. Chem. Phys. 1998, **109** , 8218; (c) R. Bauernschmitt and R. Ahlrichs, Chem. Phys. Lett. 1996, **256**, 454.
40 (a) T. Liu, H.X. Zhang and B.H. Xia, J. Phys. Chem. A 2007, **111** , 8724; (b) X. Zhou, H.X. Zhang, Q.J. Pan, B.H. Xia and A.C. Tang, J. Phys. Chem. A 2005, **109**, 8809; (c) X. Zhou, A.M. Ren and J.K. Feng, J. Organomet. Chem. 2005, **690**, 338. (d) A. Albertino, C. Garino, S. Ghiani, R. Gobetto, C. Nervi, L. Salassa, E. Rosenverg, A. Sharmin, G. Viscardi, R. Buscaino, G. Cross and M. Milanesio, J. Organomet. Chem. 2007, **692**, 1377.
41 M. J. Frisch, G. W. Trucks, H. B. Schlegel, G. E. Scuseria, M. A. Robb, J. R. Cheeseman, G. Scalmani, V. Barone, B. Mennucci, G. A. Petersson, H. Nakatsuji, M. Caricato, X. Li, H. P. Hratchian, A. F. Izmaylov, J. Bloino, G. Zheng, J. L. Sonnenberg, M. Hada, M. Ehara, K. Toyota, R. Fukuda, J. Hasegawa, M. Ishida, T. Nakajima, Y. Honda, O. Kitao, H. Nakai, T. Vreven, J. A. Montgomery Jr., J. E. Peralta, F. Ogliaro, M. Bearpark, J. J. Heyd, E. Brothers, K. N. Kudin, V. N. Staroverov, R. Kobayashi, J. Normand, K. Raghavachari, A. Rendell, J. C. Burant, S. S. Iyengar, J. Tomasi, M. Cossi, N. Rega, J. M. Millam, M. Klene, J. E. Knox, J. B. Cross, V. Bakken, C. Adamo, J. Jaramillo, R. Gomperts, R. E. Stratmann, O. Yazyev, A. J. Austin, R. Cammi, C. Pomelli, J. W. Ochterski, R. L. Martin, K. Morokuma, V. G. Zakrzewski, G. A. Voth, P. Salvador, J. J. Dannenberg, S. Dapprich, A. D. Daniels, Ö. Farkas, J. B. Foresman, J. V. Ortiz , J. Cioslowski and D.J. Fox, Gaussian 09, (Revision A.1), Gaussian, Inc., Wallingford, CT 2009.

42 N. M. O'Boyle, A. L. Tenderholt and K. M. Langner, J. Comp.Chem. 2008, **29**,839.

43 R. Alam, T. Mistri, A. Katarkar, K. Chaudhuri, S. K. Mandal, A. R. Khuda-Bukhsh, K.K. Das and M. Ali, Analyst, 2014, **139**, 4022.

A novel pyrene-2-(pyridin-2-ylmethylsulfanyl)ethylamine based turn-on dual sensor for Al^{3+}: experimental and computational studies†

Rahul Bhowmick[a], Malay Dolai[a], Rabiul Alam[a], Tarun Mistri[a], Atul Katarkar[b], Keya Chaudhuri[b] and Mahammad Ali[a]*

A pyrene based pyrene-2-(Pyridin-2-ylmethylsulfanyl)-ethylamine (PP) is found to exhibit a turn-on chemo- and fluorogenic dual sensing of Al^{3+}, through PET blocking and CHEF effect.